Title

Synthesis of Silver Nanowires with Reduced Diameters Using Benzoin-Derived Radicals to Make Transparent Conductors with High Transparency and Low Haze

Journal

Nano Letters, 18(8)

ISSN

1530-6984

Authors

Niu, Zhiqiang
Cui, Fan
Kuttner, Elisabeth
et al.

Publication Date

2018-08-08

DOI

10.1021/acs.nanolett.8b02479

Peer reviewed

NANO LETTERS
Letter
Cite This: Nano Lett. 2018, 18, 5329−5334
pubs.acs.org/NanoLett

Synthesis of Silver Nanowires with Reduced Diameters Using Benzoin-Derived Radicals to Make Transparent Conductors with High Transparency and Low Haze

Zhiqiang Niu,[†,‡,¶] Fan Cui,[†,‡,¶] Elisabeth Kuttner,[∥] Chenlu Xie,[†] Hong Chen,[†] Yuchun Sun,[†] Ahmad Dehestani,[‡] Kerstin Schierle-Arndt,[‡] and Peidong Yang*[,†,‡,§,⊥,#]

[†]Department of Chemistry, University of California, Berkeley, California 94720, United States
[‡]California Research Alliance (CARA), BASF Corporation, Berkeley, California 94720, United States
[∥]BASF Corporation, Ludwigshafen am Rhein 67056, Germany
[§]Materials Sciences Division, Lawrence Berkeley National Laboratory, Berkeley, California 94720, United States
[⊥]Department of Materials Science and Engineering, University of California, Berkeley, California 94720, United States
[#]Kavli Energy NanoSciences Institute, Berkeley, California 94720, United States

Supporting Information

ABSTRACT: Reducing the diameter of silver nanowires has been proven to be an effective way to improve their optoelectronic performance by lessening light attenuation. The state-of-the-art silver nanowires are typically around 20 nm in diameter. Herein we report a modified polyol synthesis of silver nanowires with average diameters as thin as 13 nm and aspect ratios up to 3000. The success of this synthesis is based on the employment of benzoin-derived radicals in the polyol approach and does not require high-pressure conditions. The strong reducing power of radicals allows the reduction of silver precursors to occur at relatively low temperatures, wherein the lateral growth of silver nanowires is restrained because of efficient surface passivation. The optoelectronic performance of as-prepared 13 nm silver nanowires presents a sheet resistance of 28 Ω sq^{-1} at a transmittance of 95% with a haze factor of ∼1.2%, comparable to that of commercial indium tin oxide (ITO).

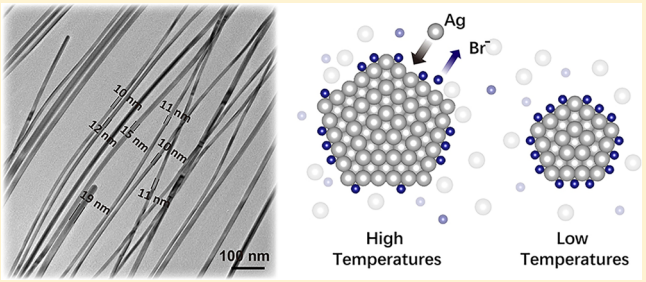

KEYWORDS: *silver nanowire, ultrathin, polyol synthesis, transparent conductor, low haze factor*

Transparent conducting films are commonly used in solar cells, organic light emitting diodes, displays, touch panels, smart windows, and so on.[1,2] Indium tin oxide (ITO) is the predominant material being used in incumbent technology.[2] However, the limited supply of indium and the high cost of manufacturing process of ITO overshadows its future domination.[3] These limitations have motivated an intensive search of alternative materials, such as carbon nanotubes,[4] graphene,[5] conducting polymers,[6] metal meshes, and metal nanowire networks.[3] Silver nanowires stand out among all the replacements. Compared to ITO, silver nanowires have better flexibility and comparable or better optoelectronic performance.[3,7,8]

The diameter and the aspect ratio of silver nanowires are two key structural traits that determine their film performance.[9] Specifically, the diameter is proportional to the magnitude of light scattering in nanowire mesh films, and the aspect ratio is correlated with the number of interwire junctions. As such, high-performance transparent electrodes require thin diameter and high aspect ratio, posing a stringent challenge to nanowire synthesis. Polyol synthesis is the most popular method to produce silver nanowires so far.[10,11] The produced silver nanowires have diameters usually larger than 50 nm. To thin down the diameters, several modified versions of polyol synthesis have been developed. The introduction of bromide ion (Br^-), which strongly binds to the Ag(100) surface, has been shown to generate wires less than 50 nm.[12,13] Later, the combined use of high-molecular-weight PVP and Br^- yielded wires around 20 nm in diameter.[14−17] A very recent study by Kim and co-workers reports an unconventional method that can achieve silver nanowires of 15 nm in diameters, but remarkably high pressure is required.[18] These thin silver nanowires have shown very promising film performance,[15,16,19] on the same level to that of ITO (50 Ω sq^{-1} with 95% transmittance).[3] Despite the progress, the synthesis of wires less than 20 nm under ambient conditions has had limited success, and the optoelectronic performance of the wires is an intriguing topic of study.

Received: June 19, 2018
Revised: July 9, 2018
Published: July 16, 2018

DOI: 10.1021/acs.nanolett.8b02479
Nano Lett. 2018, 18, 5329−5334

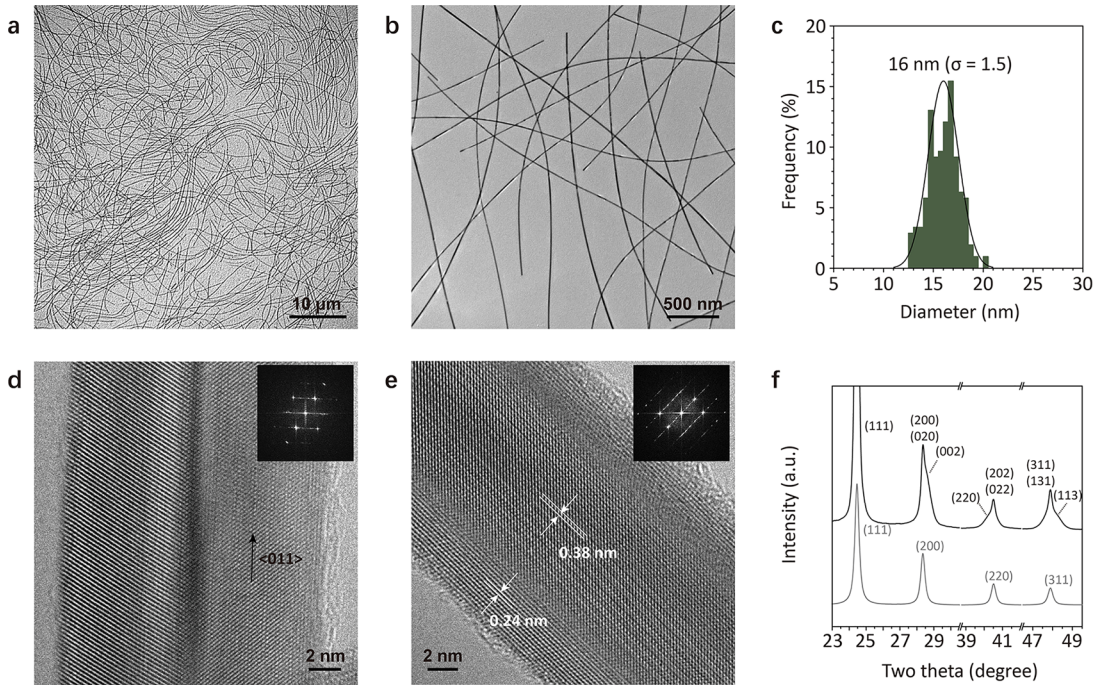

Figure 1. Silver nanowires (16 nm in diameter) prepared by incorporating benzoin into a standard polyol synthesis. (a,b) TEM images with different magnifications; (c) diameter histogram; (d,e) HRTEM images with corresponding fast Fourier transformations (FFT) in insets; (f) experimental XRD pattern (black curve) and simulated XRD pattern of a fcc phase (gray curve). The peak splitting is a result of anisotropic lattice distortions in the twinned structure with high internal strains.

The diameter of silver nanowires can be modified by adjusting reduction kinetics.[17] In polyol synthesis, the reductants are from the decomposition of ethylene glycol (EG) at elevated temperature.[20] However, the temperature-dependent decomposition of EG compromises the tunability of this method, especially in the low-temperature zone. Adding external reductants is a possible way to address this issue. Given that all the chemical species in a polyol synthesis are interconnected, an appropriate foreign reductant should not disturb this delicate chemical network. Our group recently reported the use of benzoin-derived radicals as generalized reducing agents to make sub-20 nm copper nanowires.[21] The mechanism studies pointed to a scenario that the radicals regulated the reduction kinetics of copper precursor. In general, benzoin is chemically stable under ambient conditions and generates reactive radicals upon exposure to heating. The reactivity of the derived radicals can be tuned by introducing electron-donating/-withdrawing groups on the two phenyl rings of benzoin.[21] In addition, this new type of reductant is compatible with hydrophilic EG. These advantages encourage us to systematically investigate the potential value of benzoin in making thin silver nanowires. Herein we report a benzoin-modified polyol synthesis of silver nanowires with sub-20 nm diameters and demonstrate their excellent film performance in terms of transparency and haze.

Our efforts to make thin silver nanowires started by incorporating benzoin into a standard polyol protocol which yields wires with diameters around 20 nm.[15] In a typical synthesis (for more details, see Experiment Section in Supporting Information), silver precursor ($AgNO_3$) and capping agent (polyvinylpyrrolidone, PVP) were mixed with halide ions (Cl^- and Br^-) in EG. The mixture was stirred at room temperature (RT) for 30 min. The solution gradually turned opaque white, suggesting the formation of insoluble silver halides (AgCl and AgBr). Then, benzoin was added into this colloidal suspension. The reaction mixture was bubbled with nitrogen (N_2) and heated from room temperature to 150 °C, 20 degrees lower than the original version. The reaction mixture was quenched 75 min after the outset of heating up. The silver nanowires were collected, purified, and characterized.

Figure 1a,b shows the transmission electron microscopy (TEM) images of the produced silver nanowires. The wires have an average diameter of 16 nm (Figure 1c, standard deviation: σ = 1.5) and lengths up to 35 μm (Figure S1). The crystal structure of the silver nanowires is characterized by high-resolution (HR) TEM (Figure 1d,e). A twin plane is shown in parallel to <110> axis (Figure 1d). It suggests that the thin nanowire has a typical 5-fold twinned structure composed of five pieces of single crystalline subunits. When the incident electron beam is perpendicular to a lateral surface of the wire, a Moiré pattern shows up in the middle with a large lattice spacing of 0.38 nm (Figure 1e). This is caused by the superimposition of upper and lower single crystalline subunits. The X-ray diffraction (XRD) pattern of the silver nanowires was recorded at Stanford Synchrotron Radiation Light Source at Beamline 2−1 by using an X-ray beam with a wavelength of 0.9765 Å. Their diffraction peaks (black curve, Figure 1f) present obvious asymmetries as compared with that of face-centered cubic (fcc) silver (gray curve, Figure 1f). A similar observation was reported previously by Sun and co-workers.[22] The peak splitting can be attributed to anisotropic lattice distortions in the twinned structure with high internal strains. Taken together, these characterizations have clearly shown that the addition of benzoin to a polyol synthesis can appreciably reduce the average diameter of silver nanowires from 20 to 16 nm. The preserved 5-fold twinned structure

DOI: 10.1021/acs.nanolett.8b02479
Nano Lett. 2018, 18, 5329−5334

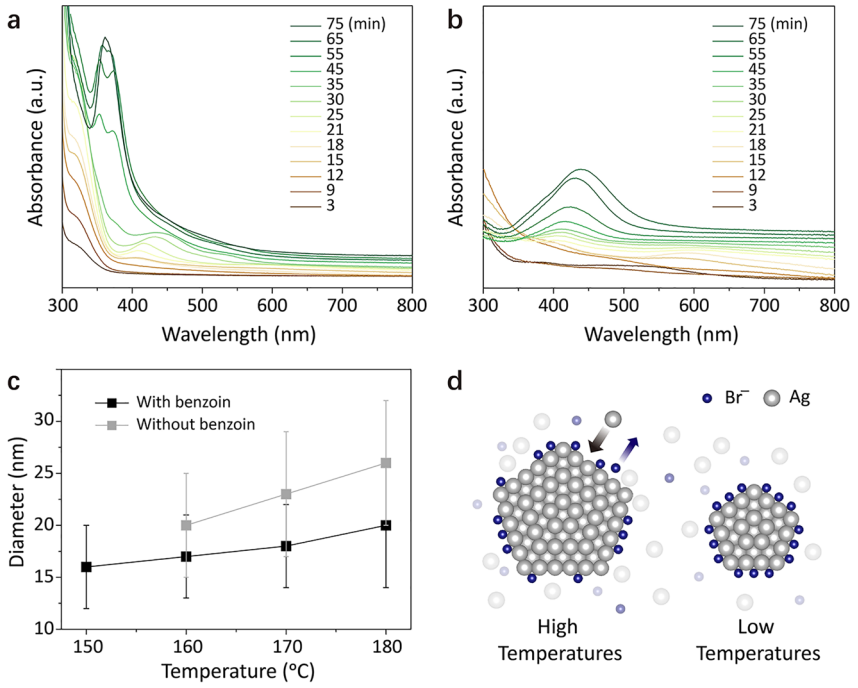

Figure 2. (a) UV−vis absorption spectra of aliquots taken from the reaction mixtures with benzoin; (b) UV−vis absorption spectra of aliquots taken from the reaction mixtures without benzoin. It shows that the addition of benzoin leads to a faster reduction rate. (c) The average diameters of silver nanowires grown at temperatures of 150−180 °C. The nanowires became thicker with the increased growth temperature, independent of the existence of benzoin. (d) Schematic illustration showing cross sections of silver nanowires grown at high temperatures and low temperatures, respectively. The Ag(100) surface is tightly bound by bromide ions at low temperatures, impeding the lateral growth.

indicates that benzoin did not interrupt the growth trajectory of silver nanowires.

To disclose the role of benzoin in making thin nanowires, we compared the reduction kinetics in polyol synthesis with and without the addition of benzoin using ultraviolet−visible (UV−vis) spectroscopy. Two respective reaction mixtures were placed in a same oil bath at RT. Right after the oil bath was set to the desired reaction temperature (150 °C), aliquots were concurrently taken from the two reaction solutions at intervals.

In the presence of benzoin, the initial products collected from the reaction solution within the first 12 min were large, irregular particles (Figure S2a,b), which were identified as silver halides (AgCl and AgBr) generated from the reaction between $AgNO_3$ and NaCl/NaBr (Figure S3a). The formation of insoluble silver halides allowed a tight control over the concentration of silver precursor in the growth solution and greatly reduced the supersaturation level of silver atoms.[12,15,17] During this period, no obvious absorption was observed in the visible region (Figure 2a). When the reaction proceeded for 15 min, a broad peak showed up at 408 nm. This peak can be assigned as the featured surface plasmon resonance (SPR) of silver nanoparticles, as evidenced by TEM (Figure S2c,d). It marks the start of the reduction of the silver precursor. This peak gradually became stronger and was accompanied by a continuous red-shift when the reaction was prolonged to 35 min. These changes can be attributed to the growing size and number of the silver particles. Meanwhile, TEM studies also reveal that one-dimensional products began to appear at 30 min (Figure S2e) and became populated at 35 min (Figure S2f). The large silver halide particles seemed to be less at this stage, and the newly formed one-dimensional structures were generally short. In response to the explosion of short wires, an absorption peak around 370 nm emerged at 35 min (Figure 2a). It further evolved to characteristic absorption of silver nanowires within the next 10 min. Two peaks at 372 and 352 nm were observed for the products collected at 45 min. They correspond to transverse SPR mode of one-dimensional silver nanostructures with a pentagonal cross-section and bulk silver, respectively.[23,24] From 45 to 75 min, the two resonance peaks grew stronger as more nanowires were produced. At the same time, they became closer to each other and eventually merged to one peak at 361 nm, suggesting the sharp pentagonal cross-section became round.[24]

In the absence of benzoin, the reduction of silver precursor was quite sluggish. The SPR peak of silver nanoparticles slowly developed in 21 min (Figure 2b). Although it continued growing thereafter, the resonance peaks of one-dimensional wires never showed up. The products at 75 min were mainly near-spherical large silver halides mixed with silver nanoparticles as evidenced by XRD (Figure S3b) and TEM (Figure S4). These results indicate that the reducing power of EG and its derivatives is not efficient to deliver silver nanowires at low temperature while keeping other conditions the same as in the standard protocol.

In fact, the reaction temperature has profound impact on the lateral growth of silver nanowires. As shown in Figure 2c, the average diameters of silver nanowires increased along with the reaction temperatures, regardless of whether benzoin was added or not. In addition, at the same growth temperatures, the diameters of the nanowires synthesized with benzoin were always thinner than those without benzoin. A plausible scenario is that the faster reduction kinetics of the benzoin system can generate more nuclei at the initial stage of one-dimensional growth, leading to less silver precursor allocated to each nuclei in the succeeding growth. On the other hand, it is

DOI: 10.1021/acs.nanolett.8b02479
Nano Lett. 2018, 18, 5329−5334

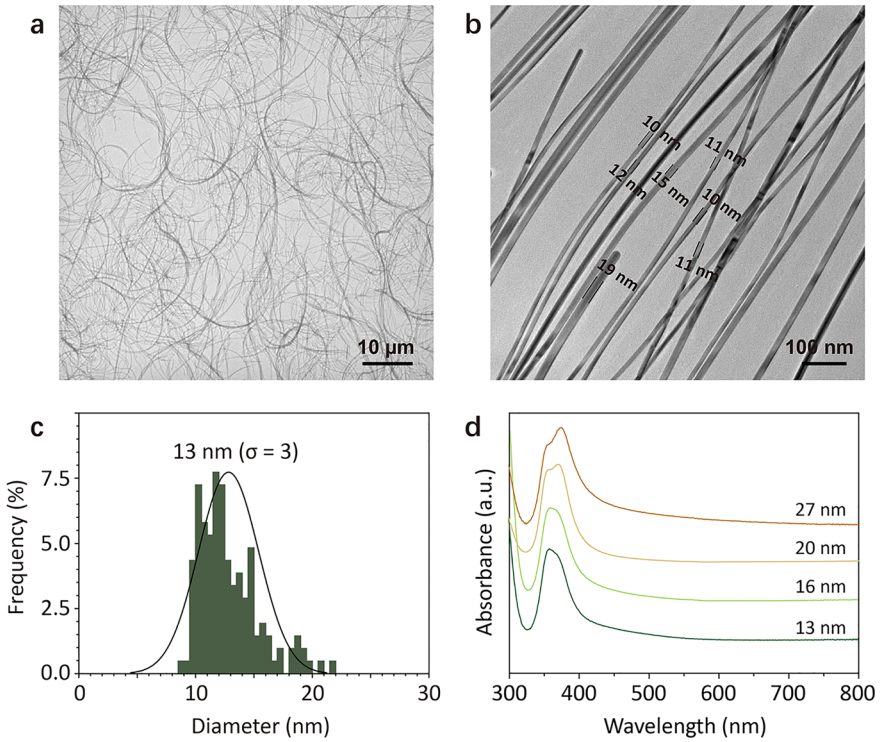

Figure 3. Silver nanowires (13 nm in diameter) synthesized using a standard procedure with optimized concentration of bromide ions. (a,b) TEM images with different magnifications; (c) diameter histogram; (d) UV−vis adsorption spectra of wires with different diameters. The two featured SPR peaks observed in silver nanowires with diameters larger than 20 nm merge into a single resonance for those with diameters of 16 and 13 nm, indicative of the smoothed surface of thinner wires.

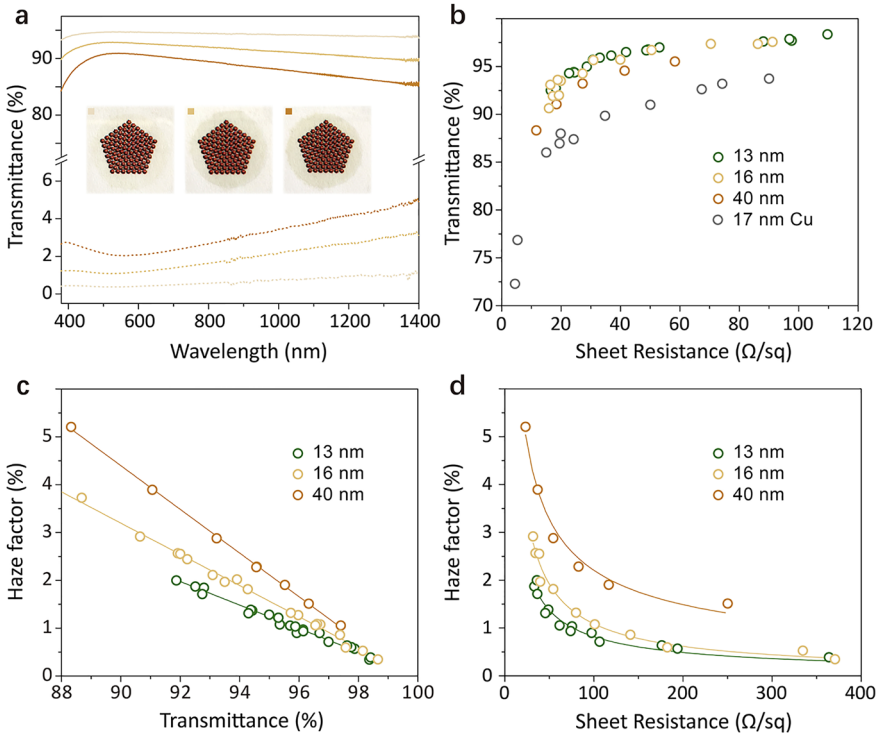

Figure 4. Optoelectronic performance of transparent conductive films. (a) transmittance (solid curve) and scattering (dashed curve) spectra of transparent conductors with different loadings of 13 nm silver nanowires. Inset shows the optical pictures of films in the corresponding cases. Plots of transmittance versus sheet resistance (b), haze factor versus transmittance (c), and haze factor versus sheet resistance (d) of electrodes made with silver nanowires with different mean diameters.

well accepted that Br^- can selectively adsorb on the lateral surface, that is, Ag(100).[25] The rate of atomic addition on Ag(100) is therefore correlated to the coverage density of bromide ions. In a study of shape-selective synthesis of

DOI: 10.1021/acs.nanolett.8b02479
Nano Lett. 2018, 18, 5329−5334

palladium nanocrystals, it has been demonstrated that the density of chemisorbed Br^- on the Pd(100) surface is inversely proportional to temperature.[26] More bromide ions are, therefore, expected on the Ag(100) surface at lower temperature, exerting more restraint on the lateral growth. As illustrated in Figure 2d, at high temperatures, the dynamic adsorption and desorption of bromide ions on Ag(100) makes the lateral surface exposed to silver species in the solution, leading to lateral growth of silver nanowires. However, at low temperatures, the desorption of bromide ions will be slowed down. It blocks the access of silver precursors to the lateral surface and yields thinner wires.

To test this hypothesis, we varied the amount of bromide ions added into the synthesis. By eliminating Br^- from the recipe, fat and short nanowires were produced (Figure S5a). Conversely, when the amount of Br^- was doubled or tripled, the diameters of as-synthesized silver nanowires became thinner than 16 nm (Figure S5b). These two control experiments unambiguously confirm that the bromide ions have significant influence over the lateral dimensions of silver nanowires. On this foundation, we further optimized the synthesis by dismissing chloride ions in the standard protocol and using bromide ions alone. As shown in Figure 3, silver nanowires with an average diameter of unprecedented 13 nm (Figure 3c) were prepared in high quality. Their length is up to 40 μm (Figure S5c), that is, aspect ratios up to 3000. Figure 3d compares the UV−vis absorption spectra of silver nanowires with different average diameters. Two separate SPR peaks were observed for silver nanowires with diameters larger than 20 nm, while they merge into a single resonance for those with diameters of 16 and 13 nm. As mentioned earlier, this is attributed to the rounded cross-section of the wires.[24] In principle, the ultrathin nanowires have relatively high surface energy, especially for corner atoms with high unsaturation. A thermal driven surface diffusion process may account for the smooth-edged ultrathin nanowires. This interpretation is supported by the shape evolution of UV−vis absorption spectra shown in Figure 2a. In addition, a blue shift was observed for the transverse SPR peak of the silver nanowires when reducing their diameters.

Transparent conducting films were fabricated using a filtration method as reported previously.[27−29] The as-made films were then subjected to an additional $NaBH_4$ treatment to improve wire-to-wire connection.[30] The insets in Figure 4a show three films with different wire (13 nm in diameter) loadings. The underlying patterns can be viewed with excellent clarity. The total transmittance (solid curve) and forward scattering (dashed curve) spectra of these three films are exhibited in Figure 4a. The silver films show high transparency and low scattering over a wide scale of wavelength. This is a general advantage of nanowire-based conductors compared with oxide-based conductors. The transmittance of light in a mesh film is enabled by structural openings which is independent of incident wavelength, while the transparency of oxide materials is usually confined within a small window of the spectrum between the margin of free electron plasma frequency and the bandgap. For the same reason, the transmittance is much less wavelength-dependent, explained by the overall flatness of the spectra shape. The thickness of the films was adjusted by varying the loading amount of silver nanowires. More light is absorbed by silver nanowires with increased film thickness, leading to smaller transmittance and larger scattering.

The transmittance−sheet resistance relationships are plotted in Figure 4b. The film performance of as-synthesized silver nanowires with three different diameters (e.g., 13 nm, 16 nm, 40 nm) were compared, with copper nanowires of 17 nm in diameter as a benchmark (data extracted from citation).[27] The ultrathin silver nanowire films show outstanding conductivity in general, significantly better than copper nanowire films made with the similar method due to silver's higher intrinsic conductivity. There is a slight enhancement in conductivity as the nanowire diameters shrink from 40 to 13 nm. This can be attributed to the increased aspect ratios due to the reduced diameters. In particular, films made by 13 nm silver nanowires present a sheet resistance of 28 Ω sq^{-1} at a transmittance of 95%. Compared with the state-of-the-art silver nanowires, this work is at the same tier of the best performance reported in the literature.[15,16,19]

Unlike homogeneously composed oxide films, the light scattering (usually quantified with haze factor, defined as forward scattering divided by total transmittance) in nanowire meshes is usually nontrivial. The nanoscopic structures can act as intensive scattering centers. Applications like displays require low light scattering to afford a sharp contrast.[3] Previous studies indicate that in the random mesh geometry, the haze factor is sensitive to nanowire diameters:[31] the thinner the wires are, the smaller the haze factor. The motivation of making ultrathin nanowires in this work is to minimize the light scattering. Figure 4c charts the variation of transmittance over haze factor for conductors made from silver nanowires with different diameters. The film fabrication methods were kept the same for all cases to eliminate process-specific inhomogeneity. Typically, in a film with 95.6% (91.8%) of total transmittance at 550 nm, the forward scattering contributes 1.24% (1.97%). As the nanowire diameter gets thinner, the haze factor significantly decreases. Figure 4d plots the haze factor as a function of sheet resistance. Remarkably, 13 nm Ag nanowires achieve less than 1% haze with sheet resistance being as low as 30 Ω sq^{-1}, among the best compared with the haze values reported in the literature.[19,32−34]

In summary, we have shown a robust synthetic protocol to reduce the diameters of silver nanowires from 20 to 16 nm by introducing an external reducing agent, benzoin, into a standard polyol approach. We studied the reduction kinetics to gain a deeper understanding of the role of benzoin. Time-dependent UV−vis absorption spectra, TEM, and XRD experiments were therefore performed to follow the chemical changes in the reaction solutions. We have proven that the strong reducing power of benzoin-derived radicals can speed up the reduction of silver precursors. It makes the growth of silver nanowires viable at relatively low temperatures, leading to more efficient surface passivation of Ag(100) by bromide ions. On this basis, by carefully optimizing the concentration of bromide ions, we were able to achieve unprecedented 13 nm silver nanowires with aspect ratios up to 3000. As presented, the diameters exert great influence on the optoelectronic performance of the corresponding transparent conductors. We have established an ascending trend of film performance with the decreased diameters. Particularly, the as-prepared 13 nm nanowires exhibit a sheet resistance of 28 Ω sq^{-1} at a transmittance of 95% with a haze factor of ~1.2%, comparable to the performance of commercial ITO. This benzoin-modified polyol synthesis exemplifies the potential of free-radical chemistry in making advanced nanostructures with enhanced performance.

DOI: 10.1021/acs.nanolett.8b02479
Nano Lett. 2018, 18, 5329−5334

■ ASSOCIATED CONTENT

Supporting Information

The Supporting Information is available free of charge on the ACS Publications website at DOI: 10.1021/acs.nanolett.8b02479.

Detailed description of experimental methods and additional figures (PDF)

■ AUTHOR INFORMATION

Corresponding Author

*E-mail: p_yang@berkeley.edu.

ORCID

Zhiqiang Niu: 0000-0002-9122-4880
Fan Cui: 0000-0003-3394-8095
Chenlu Xie: 0000-0001-9215-6878
Hong Chen: 0000-0003-4053-7147
Peidong Yang: 0000-0003-4799-1684

Author Contributions

¶Z.N. and F.C. contributed equally to this work.

Notes

The authors declare no competing financial interest.

■ ACKNOWLEDGMENTS

This work was financially supported by BASF Corporation (Award Number 84428967). Work at the NCEM, the Molecular Foundry and the Advanced Light Source was supported by the Director, Office of Science, Office of Basic Energy Sciences, of the U.S. Department of Energy under Contract No. DE-AC02-05CH11231. The research used the resource at the Stanford Synchrotron Radiation Light Source at SLAC National Accelerator Laboratory supported by the U.S. Department of Energy, Office of Science, Basic Energy Sciences under contract no. DE-AC02-76SF00515.

■ REFERENCES

(1) *Handbook of Transparent Conductors*Hosono, H., Paine, D. C., Ginley, D., Eds.; Springer Science & Business Media, 2010.
(2) Ghaffarzadeh, K.; Das, R. *Transparent Conductive Films (TCF) 2016–2026: Forecasts, Markets, Technologies*; IDTechEx, 2016.
(3) Ye, S. R.; Rathmell, A. R.; Chen, Z. F.; Stewart, I. E.; Wiley, B. J. *Adv. Mater.* **2014**, *26*, 6670–6687.
(4) Wu, Z.; Chen, Z.; Du, X.; Logan, J. M.; Sippel, J.; Nikolou, M.; Kamaras, K.; Reynolds, J. R.; Tanner, D. B.; Hebard, A. F. *Science* **2004**, *305*, 1273–1276.
(5) Li, X.; Zhu, Y.; Cai, W.; Borysiak, M.; Han, B.; Chen, D.; Piner, R. D.; Colombo, L.; Ruoff, R. S. *Nano Lett.* **2009**, *9*, 4359–4363.
(6) Na, S. I.; Kim, S. S.; Jo, J.; Kim, D. Y. *Adv. Mater.* **2008**, *20*, 4061–4067.
(7) De, S.; Higgins, T. M.; Lyons, P. E.; Doherty, E. M.; Nirmalraj, P. N.; Blau, W. J.; Boland, J. J.; Coleman, J. N. *ACS Nano* **2009**, *3*, 1767–1774.
(8) Langley, D.; Giusti, G.; Mayousse, C.; Celle, C.; Bellet, D.; Simonato, J. P. *Nanotechnology* **2013**, *24*, 452001.
(9) Mutiso, R. M.; Sherrott, M. C.; Rathmell, A. R.; Wiley, B. J.; Winey, K. I. *ACS Nano* **2013**, *7*, 7654–7663.
(10) Sun, Y.; Yin, Y.; Mayers, B. T.; Herricks, T.; Xia, Y. *Chem. Mater.* **2002**, *14*, 4736–4745.
(11) Sun, Y.; Xia, Y. *Adv. Mater.* **2002**, *14*, 833–837.
(12) Hu, L.; Kim, H. S.; Lee, J.-Y.; Peumans, P.; Cui, Y. *ACS Nano* **2010**, *4*, 2955–2963.
(13) Zhang, K.; Du, Y.; Chen, S. *Org. Electron.* **2015**, *26*, 380–385.
(14) Lee, E.-J.; Chang, M.-H.; Kim, Y.-S.; Kim, J.-Y. *APL Mater.* **2013**, *1*, 042118.
(15) Li, B.; Ye, S.; Stewart, I. E.; Alvarez, S.; Wiley, B. J. *Nano Lett.* **2015**, *15*, 6722–6726.
(16) Lee, E.-J.; Kim, Y.-H.; Hwang, D. K.; Choi, W. K.; Kim, J.-Y. *RSC Adv.* **2016**, *6*, 11702–11710.
(17) da Silva, R. R.; Yang, M.; Choi, S.-I.; Chi, M.; Luo, M.; Zhang, C.; Li, Z.-Y.; Camargo, P. H.; Ribeiro, S. J. L.; Xia, Y. *ACS Nano* **2016**, *10*, 7892–7900.
(18) Jang, H.-W.; Kim, Y.-H.; Lee, K.-W.; Kim, Y.-M.; Kim, J.-Y. *APL Mater.* **2017**, *5*, 080701.
(19) Menamparambath, M. M.; Yang, K.; Kim, H. H.; Bae, O. S.; Jeong, M. S.; Choi, J. Y.; Baik, S. *Nanotechnology* **2016**, *27*, 465706.
(20) Skrabalak, S. E.; Wiley, B. J.; Kim, M.; Formo, E. V.; Xia, Y. *Nano Lett.* **2008**, *8*, 2077–2081.
(21) Cui, F.; Dou, L.; Yang, Q.; Yu, Y.; Niu, Z.; Sun, Y.; Liu, H.; Dehestani, A.; Schierle-Arndt, K.; Yang, P. *J. Am. Chem. Soc.* **2017**, *139*, 3027–3032.
(22) Sun, Y.; Ren, Y.; Liu, Y.; Wen, J.; Okasinski, J. S.; Miller, D. J. *Nat. Commun.* **2012**, *3*, 971.
(23) Kelly, K. L.; Coronado, E.; Zhao, L. L.; Schatz, G. C. *J. Phys. Chem. B* **2003**, *107*, 668–677.
(24) Hwang, J.; Lee, H.; Woo, Y. *J. Appl. Phys.* **2016**, *120*, 174903.
(25) Wiley, B.; Sun, Y.; Xia, Y. *Acc. Chem. Res.* **2007**, *40*, 1067–1076.
(26) Peng, H.-C.; Xie, S.; Park, J.; Xia, X.; Xia, Y. *J. Am. Chem. Soc.* **2013**, *135*, 3780–3783.
(27) Cui, F.; Yu, Y.; Dou, L.; Sun, J.; Yang, Q.; Schildknecht, C.; Schierle-Arndt, K.; Yang, P. *Nano Lett.* **2015**, *15*, 7610–7615.
(28) Dou, L.; Cui, F.; Yu, Y.; Khanarian, G.; Eaton, S. W.; Yang, Q.; Resasco, J.; Schildknecht, C.; Schierle-Arndt, K.; Yang, P. *ACS Nano* **2016**, *10*, 2600–2606.
(29) Niu, Z.; Cui, F.; Yu, Y.; Becknell, N.; Sun, Y.; Khanarian, G.; Kim, D.; Dou, L.; Dehestani, A.; Schierle-Arndt, K.; Yang, P. *J. Am. Chem. Soc.* **2017**, *139*, 7348–7354.
(30) Ge, Y.; Duan, X.; Zhang, M.; Mei, L.; Hu, J.; Hu, W.; Duan, X. *J. Am. Chem. Soc.* **2018**, *140*, 193–199.
(31) Khanarian, G.; Joo, J.; Liu, X.-Q.; Eastman, P.; Werner, D.; O'Connell, K.; Trefonas, P. *J. Appl. Phys.* **2013**, *114*, 024302.
(32) Menamparambath, M. M.; Ajmal, C. M.; Kim, K. H.; Yang, D.; Roh, J.; Park, H. C.; Kwak, C.; Choi, J.-Y.; Baik, S. *Sci. Rep.* **2015**, *5*, 16371.
(33) Araki, T.; Jiu, J.; Nogi, M.; Koga, H.; Nagao, S.; Sugahara, T.; Suganuma, K. *Nano Res.* **2014**, *7*, 236–245.
(34) Han, H. J.; Choi, Y. C.; Han, J. H. *Synth. Met.* **2015**, *199*, 219–222.

DOI: 10.1021/acs.nanolett.8b02479
Nano Lett. 2018, 18, 5329–5334